J. Micromech. Microeng. **16** (2006) 1935–1942 doi:10.1088/0960-1317/16/10/004

A multi-ink linear array of nanofountain probes

N Moldovan, K-H Kim and H D Espinosa

Northwestern University, 2145 Sheridan Road Evanston, IL 60208, USA

E-mail: espinosa@northwestern.edu

Received 3 May 2006, in final form 8 July 2006
Published 11 August 2006
Online at stacks.iop.org/JMM/16/1935

Abstract
After the successful design and fabrication of a single-probe nanofountain pen, a second-generation device with two on-chip ink reservoirs feeding a linear array of 12 microfluidic cantilever probes was manufactured. The new device excels by sharper and more uniform tips, more robust fabrication and improved performance in writing and imaging. Its capabilities in writing sub-100 nm features and with two different inks delivered in liquid phase were demonstrated. Their applications range from an affordable method of nanopatterning with sub-100 nm resolution to microspotters for bio-assay generation and tools for combinatorial nanoscale biochemical experiments.

(Some figures in this article are in colour only in the electronic version)

1. Introduction

Nanofountain probes (NFPs) [1–4] are atomic force microscopy (AFM) probes capable of writing by contact mode delivery of molecular inks to selected types of substrates, with a continuous microfluidic connection to on-chip or remote ink reservoirs. Historically, but also technically, they developed as enhancements to the dip-pen nanolithography (DPN) technique [5], extending its capabilities from coat-and-write to a continuous ink delivery mode of writing. NFP patterning preserves the writing finesse of DPN (typical features were sub-100 nm; the best reported: 10 nm lines and 5 nm spacing [5] (part 2)) by using the same ink delivery mechanism: the dislocation of physisorbed on-tip molecules by a small capillary condensation water meniscus formed between the tip and the substrate, the transfer of the ink molecules to the substrate by this meniscus and their subsequent surface diffusion and assembly.

We recently reported a first-generation exploratory microfabricated NFP chip capable of writing with a sub-100 nm resolution; line widths as small as 45 nm have been achieved [1, 2]. These NFP chips had a single on-chip reservoir and five cantilever probes of different lengths, with volcano-shaped ink delivery tips. The chips were designed to use only one probe at a time. The exploratory NFP chips not only demonstrated continuous ink feeding over relatively long microchannels (up to 1.35 mm in length), but also exposed fabrication difficulties and possible failure modes. These included: difficulties in channel sealing which occasionally resulted in the leaking of the channels; easy clogging of the microchannels due to their small lumen size; difficulty in controlling the cantilever bending induced by residual stresses in their composite structure; low cantilever torsional stiffness and a small reflective area leading to poor signals in the AFM optical lever detectors; difficulties in achieving the connections between the channels and volcano tips and a loose management of wafer real estate due to the KOH release of the chips. Although the re-inking time was spared, these drawbacks added to the lengthy writing process. It is known that single-probe NFP patterning, like the DPN method, is a slow process due to the diffusion-driven dissipation of molecules on the substrate surface [6] and the fact that it is a sequential type of process. The difficulties were analyzed and overcome through enhancements provided by a newly designed device and fabrication sequence. The new generation NFP chip which we present here contains a linear array of 12 cantilever probes with microfluidic channels connecting two on-chip reservoirs to volcano-shaped ink delivering tips. The 12 probes can be used in parallel, thus accelerating the writing process, but can be also fed with two different inks. To increase the success rate and usage of each chip, a similar array of probes and reservoirs are placed on both sides of the chip (figure 1). This was not possible with the old version of the NFP. The design and fabrication of the novel, second-generation NFP chip are presented in section 2. Various tests on the operation and performance of the device are presented in section 3 and

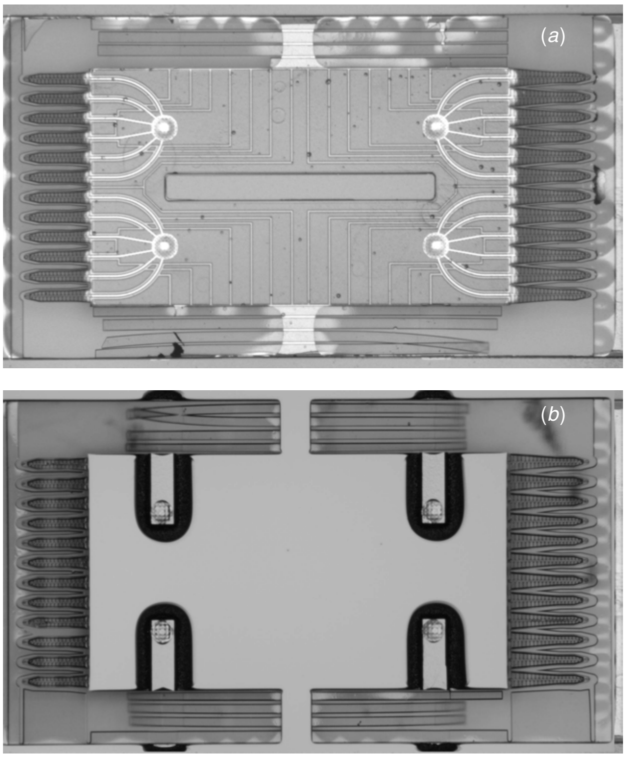

Figure 1. Chip overview: (*a*) front side view, (*b*) backside view. The chip is shown attached to the Si wafer by a pair of Si bridges with notches at their base, for controlled separation from the wafer. In both images the 520 μm long cantilevers are on the left side and the 630 μm long ones, on the right side. The long cantilever strips attached to the Si bridges are Si_3N_4 dummy structures introduced for better control of etching and mechanical tests.

discussed in section 4, where we also give an outlook to the future applications and device developments.

Since the development of our first-generation NFP, serious progress has been made and reported worldwide in the quest to develop and expedite the AFM-based patterning process. Notably, the formation of a water meniscus at the tip–substrate interface in DPN was proven by imaging the meniscus in an environmental scanning electron microscope (SEM) [7]. Several attempts were made to parallelize the writing process by developing linear [8] and 2D arrays of probes [9]. Multiple-ink writing with chips containing multiple DPN probes dipped in different solutions was tested and proven functional [10]. Several microfluidic single-probe fountain pens were reported with various designs, including closed channel devices [4] and open channel devices (microspotters) [11], with micron patterning resolution. The speed of DPN writing was increased to more than 10 μm s^{-1} by applying a voltage between the tip and substrates in particular writing schemes, such as in the electro pen nanolithography (EPN) approach [12], which achieved a 50 nm resolution. Nevertheless, some trends remained unchanged: arraying the non-microfluidic (DPN) probes allows several inks to be used, provided a multi-ink dipping system is employed. It also increases the writing speed by parallelization, although it is more difficult to align an array of probes instead of a single probe. It is also difficult to realign them and initiate writing after re-inking. Furthermore, with the exception of our first-generation NFP, the microfluidic probes reported thus far are neither capable of sub-micron writing resolution, usually due to the formation of an outer meniscus, nor do they demonstrate arraying and multiple ink delivery capabilities.

Our new generation NFP has a sub-100 nm writing resolution, demonstrates the advantages of arraying and parallel writing with multiple inks, and, unlike most other reported patterning probes, has closed channels which prevents fast evaporation and cross contamination. EPN can be easily implemented by coating the probes with metals or by integrating conductive materials into the tip. Ultrahard materials for probes, such as silicon carbide or diamond [13] can also be easily integrated.

2. Design and fabrication

A general view of the NFP device can be seen in figure 1. The chip has an overall size of 1.8 mm $\times$ 3.2 mm (excluding the cantilever lengths), to fit easily in commercial AFM equipment. The cantilever lengths are 630 μm and 520 μm, respectively for the two sides of the chip. The different lengths account for a longitudinal bending stiffness of 0.175 N m^{-1} and 0.312 N m^{-1} respectively, to provide a choice for different applications. Otherwise, the chip has a double mirroring symmetry, and an as uniform as possible and repetitive architecture, to reduce the burden of optimizing the fabrication processes for a large variety of features. Each of the reservoirs feed six microchannels. The microchannels are hosted in part on the silicon chip body, while over 630 (or 520) μm they share the length with the silicon nitride cantilevers in which they are embedded.

The total lengths of the microchannels are 1110 (1000) μm, 1175 (1055) μm and 1310 (1200) μm, respectively, for the three sets of channels symmetrically surrounding the reservoir and on the two sides of the chip. Figure 2 presents an enlarged view of a quarter of the chip, where the different components can be identified.

The microchannels have a rectangular cross section, with a height of 0.5 μm and a width of 12 μm. The reservoirs consist of two sandwiched silicon nitride membranes separated by a 0.5 μm gap and a cylindrical communication well 160 μm in diameter. The lower membrane is a sieve containing 3 μm diameter orifices, communicating with the well. The well is etched through the wafer from the backside of the chip, to reach this perforated membrane. The volume of the on-chip reservoir is given mainly by this cylindrical well and is $\sim$60 nl. The cylindrical well opens on the backside of the chip into a trapezoidal trench 40 μm deep and 220 μm wide on the wafer surface, extending from the reservoir to the margin of the chip, over a total length of 965 μm. This trench is designed to host a 100 μm diameter capillary which can be used to connect the on-chip reservoir to an even larger, remote reservoir (figures 1(*b*) and 4(*h*)). In this case, the capillary must be glued and capped with a thin counterplate with similar trenches to cover the whole backside of the chip. In a different mounting scheme without capillaries, the backside of the chip can be simply capped with a flat cover, in which case the volume of the trench can be regarded as part of a larger on-chip reservoir. All the experiments in the present study were done by feeding the ink solutions with a micropipette directly

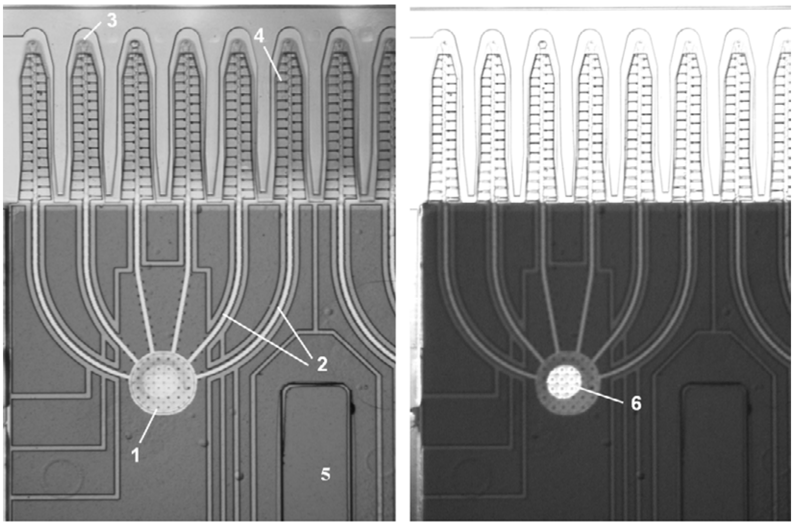

Figure 2. Enlarged view of a quarter of the NFP chip in combined reflected and transmitted light optical microscopy: (*a*) top view with more reflected light; (*b*) top view with more transmitted light, showing the reservoir well. **1**—reservoir membrane; **2**—microchannels; **3**—tip; **4**—stabilization beam; **5**—central spacing post and **6**—reservoir well.

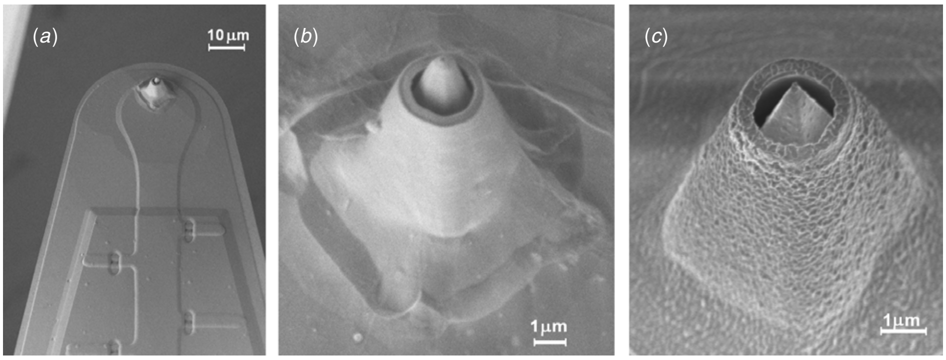

Figure 3. Volcano ink dispensing tips: (*a*) view from the cantilever end; (*b*, *c*) tip details.

into the reservoir from the backside of the chip, without the use of the capillary and capping plate. The other side of each microchannel opens into a volcano-shaped dispensing tip with a height of 7–8.5 μm, at the end of the cantilever (figure 3). The radius of the tips varies from the thickness of the lower thin nitride film (~300 nm) molded around the convex Si precursor (figure 3(*b*)), to tens of nm (figure 3(*c*)). The latter was achieved by a sharpening process that occurred with prolonged CF_4-RIE etching after removal of the top nitride. The off-center position of the core tip seen in figure 3(*b*) is an effect of reversible deformation of the structures that has been regularly observed live during the charging produced by SEM imaging. The highly compliant structure of the tip is beneficial to the writing process and may lead to a mechanism similar to the rapidograph writing nibs.

The front side of the chip is provided with a central rectangular post (figure 2, item 5) 9–10 μm thick, to prevent damage to the reservoir membranes when mounting the chip under the spring clamps of AFM heads. In the case electrodes are present on the chip, as is planned for future applications such as EPN or actuated probes, this also prevents their short circuiting.

The fabrication of the device began with the formation of silicon tips on a silicon wafer by underetching SiO_2 precursor caps in KOH to form {1 1 4}-faceted pyramids. These were further etched by a hydrofluoric–nitric–acetic acid isotropic etchant to detach the caps and sharpen the resulting tips. This process is identical to that used and optimized for the first-generation NFP [2]. The etching for tips formation also produced the central mesa structure used as a spacer in the AFM mount and recessed the active chip surface about 9 μm below the wafer surface. This prevented damage to the tips in the later lithographic processes and wafer handling, but made it necessary to perform all subsequent optical lithography processes with relatively thick photoresist (7–12 μm of Shipley SPR 220-7). This imposed optimized resist processing with special care for high aspect ratio structures and side wall profiles.

A first layer of 300–350 nm thick low stress Si_3N_4 obtained by low pressure chemical vapor deposition (LPCVD) was then deposited, followed by lithographic patterning on the backside of the wafer. This formed the rectangular windows for etching the trapezoidal trenches for the attachment of the capillaries (figure 1(*b*)). The process flow in a cross section of the reservoir area can be followed in figure 4. KOH etching of these trenches was subsequently performed for a depth of ~40 μm (figure 4(*a*)). The front side nitride was then patterned by CF_4 reactive ion etching (RIE) to outline the cantilevers

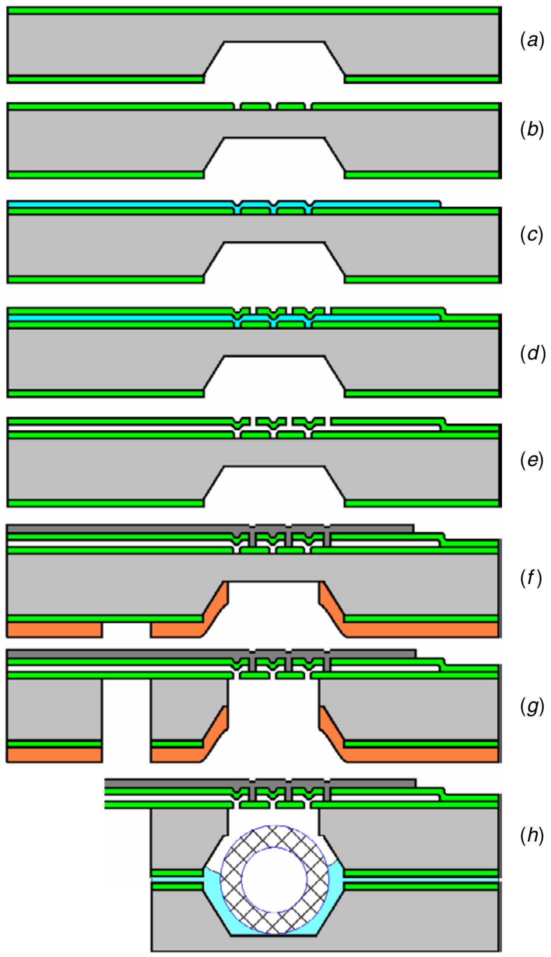

Figure 4. Fabrication sequence of the NFP chip after the Si tip formation—the reservoir area: (*a*) Si_3N_4 deposition, backside lithography and backside KOH trench formation; (*b*) front side lithography for cantilever and connection holes delineation; (*c*) PECVD SiO_2 deposition and patterning for channel core and reservoir delineation; (*d*) LPCVD of low stress nitride and patterning, resist deposition on front side and etching of protruding tips (not shown); (*e*) etching of the SiO_2 sacrificial layer; (*f*) PECVD of the SiO_2 sealing layer on the front side and thick resist lithography on the backside of the wafer; (*g*) formation of reservoir wells and chips by DRIE of Si and (*h*) schematic showing the mounting of a capillary tube with a glued counter plate, fabricated with a mask and process similar to that used in sequence (*a*) followed by dicing. Drawings are not at scale.

and the chip body. The pattern also contained an array of 3 μm diameter holes at the location of the future reservoir, forming a sieve that would later connect the microchannels to the reservoir wells (figure 4(*b*)). This bottom nitride layer made a conformal coverage of the Si pyramids and formed the tip material. A 500 nm thick SiO_2 layer was then deposited by low-temperature plasma-enhanced CVD (PECVD) at 200 °C, and patterned to form the microchannel core sacrificial layer (figure 4(*c*)). Besides the path of the microchannel lumen and reservoir, the SiO_2 pattern also contained lateral beams all along the microchannels (details visible in figure 5). These beams played a dual role: first, they provided the place where the sacrificial material would later be contacted and removed while minimizing the sealing perimeter; second, they stiffened the cantilevers for lateral bending or torsion, while maintaining a low longitudinal bending stiffness. This solution was adopted to improve upon the former generation NFP, while keeping the longitudinal cantilever stiffness in the desired range. The reflective area of the cantilevers was also increased to provide a stronger reflected light signal for the optical lever detector.

The deposition of the top Si_3N_4 layer (500 nm, low stress LPCVD) was followed by lithographic patterning to enclose the formerly delineated cantilevers and the SiO_2 pattern. Small openings (2 μm × 3 μm) were provided across the base of the aforementioned SiO_2 beams, and an array of 3 μm diameter holes was also formed in the reservoir area, symmetrically intercalated with the similar holes made in the first nitride layer (figure 4(*d*)). Etching of these features on the top Si_3N_4 layer was performed by CF_4-RIE through a thick (10 μm) photoresist mask, preventing an attack on the tips. This photoresist was removed and replaced by a 5 μm thick photoresist, through which the tips protruded about 2–3 μm. A CF_4+O_2 RIE was performed to remove the nitride from the top part of the tips, exposing the SiO_2 layer. In variations of this process used to achieve sharp tip geometries as in figure 3(*c*), the etching was prolonged until the SiO_2 layer at the tips was completely penetrated, and continued for a slight etching of the bottom nitride layer. After these processes, the photoresist was removed and a buffered oxide etch (BOE 10:1) was performed for about 400 min to completely remove the sacrificial SiO_2 layer (figure 4(*e*)). During this process, a slight attack on Si_3N_4 is believed to have occurred, leading to a thinning of the nitride, especially in the portions where the material was exposed from both sides and for a longer time, such as in the channels and at the tips. This may have contributed to an additional sharpening of the tips. To prevent the collapse of the double nitride membrane in the reservoir region and the channels in general, supercritical CO_2 drying was used after every wet process following this step.

The fabrication continued with the deposition of an SiO_2 layer (~1.5 μm, low-temperature PECVD) to completely seal the holes through which the channels and the reservoirs were cleared from the sacrificial material (figure 4(*f*)). Since minimal deposition conformity was desired to prevent the reduction of the channel lumen size, the temperature in the PECVD process was reduced to as low as 150 °C. This also produced a material with a residual stress similar to that of low stress silicon nitride (~180 MPa tensile), causing the cantilevers to remain reasonably straight after release. The sealing film was patterned lithographically by wet etching (BOE) to remove it from certain areas including the tip region, such that a complete sealing along the channels and reservoirs was preserved, while making the tip orifice communicate with the channels. At this step, the tip–channel–reservoir communication could be proven by observing water motion and evaporation under a microscope, as described in the next section (figure 5).

The process continued by deep RIE (DRIE, Bosch process) on the backside of the wafer, through a 9 μm thick photoresist layer patterned with the reservoir wells and the chip delineation pattern. This photoresist was UV-hardened and baked for 9 h at 80 °C, to prevent its reflow. Reflow prevention is particularly critical in the well region since the

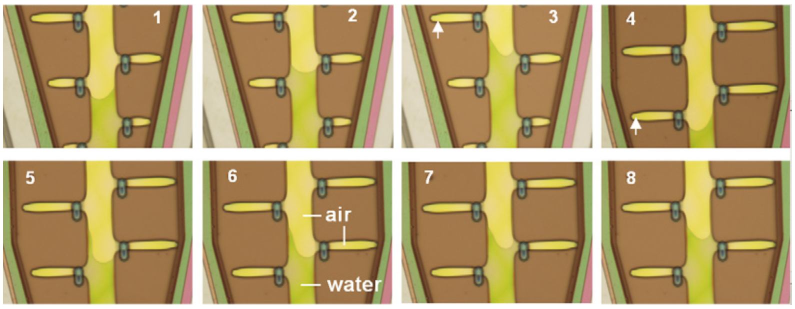

Figure 5. Snapshots of a movie showing the motion of water (darker tint) inside the sealed microchannels. There is no penetration of water from the central channel into the side beams, confirming a correct sealing. After snapshot 3, the sample was moved such that the upper left beam in frames 1–3 becomes the lower left beam in frames 4–8. The time spacing between the frames is ~1 s.

wells are in the deeply recessed area of the trapezoidal trenches for the capillary connections. This imposed restrictions on the lithographic process. Since the DRIE process is highly sensitive to the area of the features, the simultaneous opening of the reservoir well while reaching the cantilevers from the backside of the wafer in the interchip space required special attention. A preliminary study conducted using dummy wafers showed that for our process complete opening of the interchip was achieved while 40 μm remained to be etched in the reservoir well, if the etching started from a flat surface. This result obviously depended on the particular wafer size (in our case 3″ wafers 380–425 μm thick), the ratio of exposed to unexposed area, the relative positioning of features, the equipment used (Unaxis SLR 770) and so on. The 40 μm 'handicap' for the large area proved reasonable for the thickness variation across our wafers.

For the etching, the 3″ device wafers were glued on 4″ handling wafers using a boron nitride-containing heat sink compound (CG-7016, AI Technology Inc.) manually applied to the front side of the NFP wafer, mainly on the Si frame area and avoiding the reservoir areas. This mounting also prevented the cessation of the etch process at the first punch-through event on the NFP wafer. The DRIE process was carried out in steps, by carefully measuring the wafer thickness and the etching depths achieved at each step. Such rigorous control was needed since Si_3N_4, although it has a lower etch rate than silicon in the Bosch process, is not an effective etch stop material and could have led to damages on the rear side of the cantilever channels. The DRIE process was stopped when the reservoir well reached the double Si_3N_4 membrane. Fine removal of Si to completely clear the backside of the cantilevers was possible in some cases using XeF_2 etching. However, this could only be carried out for a limited time, since after ~30 min of etching, damages on Si_3N_4 could be noted. Nevertheless, XeF_2 etching was not necessary in most cases.

The use of DRIE rather than KOH etching for the chip release and reservoir formation was motivated by the small amount of space available on the chip to fit two reservoirs, given that the NFP chip should be of a standard size to fit on conventional AFM heads. DRIE also allowed more chips to be fabricated on each wafer by eliminating the space-consuming tilted walls and convex corner compensation beams in the interchip space required by the KOH process [2].

After completing the etching, the NFP wafers were detached from the handling wafers in a hot Nanostrip solution (Cyantek Co.) by careful lateral sliding and kept in the solution until complete cleaning of the boron nitride–silicone heat sink compound. DI water and methanol rinsing followed and supercritical CO_2 drying completed the process. At this step, the NFP chips remained attached to an Si frame for easy handling, as shown in figure 1. The NFP wafers then underwent a gold sputtering (~20 nm) on the backside, to enhance the reflectivity of the cantilevers (not shown in figure 1).

The released cantilevers were bent in the direction opposite to the tip for about 10 μm at their end, which was within the range easily compensated by mounting the chip at a 15° tilt in the AFM head.

3. Testing the device

The communication between the reservoir, channels and volcano dispensing tips could be checked after etching the sacrificial oxide layer and performing the sealing, by observing the motion of water due to capillarity and evaporation under an optical microscope (figure 5 and supporting material[1]). In this case, water was fed into the channels by placing a droplet onto a volcano tip using a micropipette. After releasing the chips, communication between the reservoir and channels was similarly tested, by feeding water into the reservoir well with a micropipette. Proper sealing could also be verified this way, by observing meniscus withdrawal (figure 5). In the case of inadequate sealing, during evaporation, the meniscus withdraws creating air bubbles originating at the leaking point. The communication from the reservoir well to the dispensing tips could also be substantiated from writing tests performed with various inks. Figure 6(*a*) presents a volcano tip after feeding 16-mercaptohexadecanoic acid (MHA) dissolved in acetonitrile as ink through the reservoir well, showing evidence of MHA deposits formed around the tip. In this case, the solvent was completely evaporated for the scanning electron microscopy (SEM) visualization. However, evidence of fluid ink persistence in the reservoir and channels for the time required to perform writing tests was also obtained. Simple timing measurements performed under a stereo microscope showed that methanol–water-based solutions in an open (uncapped) reservoir well take 10–30 min to completely evaporate. The capillarity

[1] Supporting material available at http://clifton.mech.northwestern.edu/~nfp/.

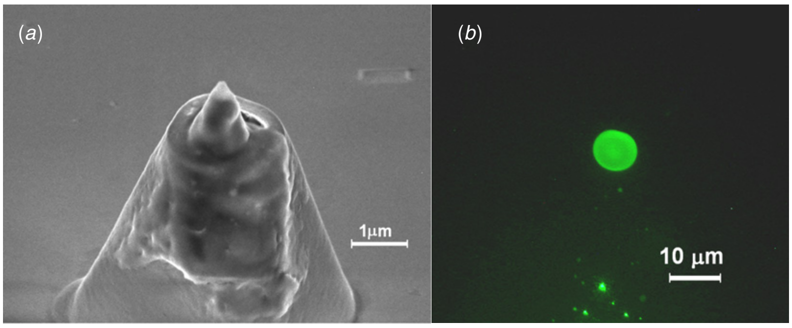

Figure 6. Evidence of connectivity and liquid ink persistence during the writing process: (*a*) SEM micrograph showing evidence of ink reflow from a volcano tip after feeding a solution of MHA into the reservoir and (*b*) 10 μm diameter MHA dot on an Au substrate as a result of puddle formation, recorded by lateral force microscopy.

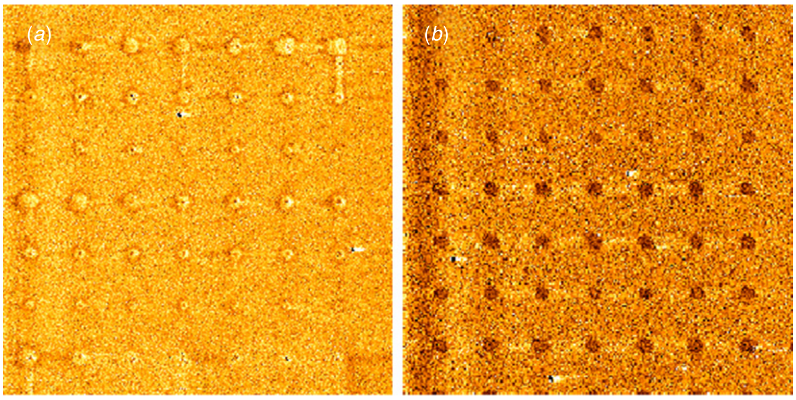

Figure 7. Dot calligraphy test with the NFP for simultaneous writing with two different inks. LFM images of areas (15 μm $\times$ 15 μm) patterned with (*a*) MHA and (*b*) PFT. Contact times were 6, 4 and 2 s for alternating rows, respectively. Relative humidity was maintained at 70 $\pm$ 5%.

dynamics keep the channels filled with liquid during this time; the channels are in fact the last to dry. In addition to this observation, there is still more direct evidence of fluid presence in the NFP system during writing. For instance, in some cases where arrays of dots of a solution containing FITC-labeled DNA were written under an applied force of 2.5 nN, a 10 μm diameter spot formed rapidly. This was a result of the ink leaking and forming an outer meniscus around the NFP tip (figure 6(*b*)). This may be linked to the higher applied force necessary for DNA patterning, although the formation of the puddle was a random occurrence.

Decidedly, the ultimate tests of the new generation NFP are the writing tests. We tested several writing protocols using thiol-based inks dissolved in acetonitrile, in conjunction with gold substrates, both in single-ink and two-ink writing modes. We present here the two-ink writing results, which are more interesting for the capabilities of this device.

Simultaneous patterning with two types of inks was performed using solutions of different thiolates. MHA and PFT (1H,1H,2H,2H-Perfluorododecane-1-thiol) were selected for testing since PFT produces dark contrast in AFM friction images while MHA gives bright contrast. We prepared saturated solutions of each in acetonitrile. One reservoir was filled with a droplet of the MHA solution while the other was filled with the PFT solution, using a micropipette. This feeding process was performed under a stereo microscope to confirm that the droplets of the two solutions did not cross contaminate. Following the feeding procedure, the chip was mounted on an AFM instrument (CP AFM, Thermomicroscopes). Since only four cantilevers could be seen by the CCD camera of the AFM at one time, the viewing field was adjusted to capture the four cantilevers from the middle of the 12 cantilever array. While the deflection of only one of the four cantilevers was monitored by the AFM feedback system, the others were passively operated and supposed to touch the substrate roughly in the same way. Once the tips were brought into contact with a gold surface, customized software was used to move the tips along the surface to pattern dot arrays. For characterization purposes, and to avoid distortion of the dot patterns by depositing new ink, the formed patterns were examined with a different probe, a commercially available silicon nitride tip for imaging. With a reference mark on the surface, the imaging tip was first positioned on an area where an MHA-fed tip had been operated. The surface was scanned to obtain a lateral force microscopy (LFM) map (figure 7(*a*)). Subsequently, the imaging tip was moved to scan a location where PFT had been patterned (figure 7(*b*)). Similar patterns were recorded for arrays of dots written with different probes of the array; however, the quality of the writing degraded with the departure from the monitored cantilever. The two ink solutions were purposely chosen to have similar writing dynamics. For instance, although separate tests showed writing capabilities with both MHA/acetonitrile and octadecanethiol (ODT)/ethanol solutions, ODT has a

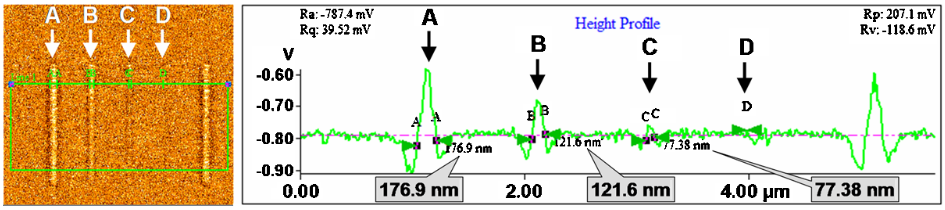

Figure 8. Line patterns written with the NFP on a gold substrate with MHA. LFM imaging was used for section analysis. The sweep rates for the unit set of lines (A, B, C and D) were 3.2, 6.4, 12.8 and 25.6 μm s^{-1}, respectively.

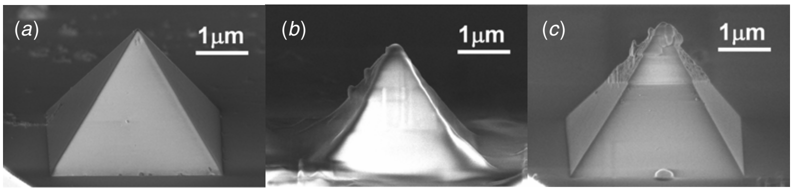

Figure 9. SEM images of a standard nitride AFM probe (*a*) before and (*b*) after dipping it in the MHA solution and drying. (*c*) Probe dipped carefully using a micromachined ink well and the AFM motion.

much lower writing speed, making its simultaneous patterning with MHA impractical.

In separate experiments NFP chips were tested for patterning lines, using the MHA solution in acetonitrile as ink. Writing proved reliable up to a writing speed of about 15 μm min^{-1}. The minimum line width obtained was ~78 nm. (figure 8).

We also demonstrated the biopatterning capability of the second-generation NFP [14]. The device is currently used in large-scale NFP patterning of DNA and various nanoparticle suspensions, the subject of further communications. Currently, studies comparing the continuous writing duration in DPN and by using the NFP are underway.

4. Discussion

Although in most DPN writing schemes ink is supplied from solutions, the ink dries up during use, forming a solid and rather irregular coating on the writing AFM probe. This aspect has not been investigated in depth thus far. Figure 9 presents an SEM view of a standard Si_3N_4 probe before (*a*) and after (*b*) dipping it into an MHA solution and drying it. Even with a careful dip performed using a micromachined ink well and the AFM head motion to achieve an initial controlled, local, partial coating [15] (figure 9(*c*)), the tip coating that develops has an irregular aspect.

This suggests that writing performed with such probes is quite different from the simplified picture that the current DPN literature proposes with regard to the meniscus-based transfer of molecules from the tip to the substrate. Even if capillary condensation plays a strong role in DPN patterning, these images suggest that writing can actually be performed at least in part like with a pencil, rather than with a quill. This explains why successful DPN writing was also performed in very dry environments and with carefully dried substrates [16]. Figure 6(*a*) shows the same type of coating on the NFP probe after solvent evaporation. Obviously, the NFP probe can be used with dry ink, as in DPN, after allowing the solvent to evaporate. In that case, the only difference would be the way in which the ink was supplied to the tip. However, in regular operation, the NFP probe has the capability of preserving the ink in liquid form during the entire patterning process. Besides the primary advantages (no re-inking interruptions), this provides the NFP with a new and slightly different mechanism of writing. For instance, the liquid present near the writing tip provides a continuous source of solvent vapors, preserving a high local solvent vapor pressure, which may contribute to the formation of a more vigorous (and chemically different) capillary condensation meniscus. Condensation of solvent vapors on the substrate is also not excluded (leading to a solvent pre-wetting layer in the vicinity of the tip) and neither is the transport of ink molecules by co-evaporation with the solvent and re-condensation. This mechanism may lead to dot-growth dynamics different from the classical DPN [6], i.e., a dot diameter growth rate on the substrate faster than that proportional to the square root of the diffusion time. Experimental investigations of these aspects are underway.

The large cross section of the NFP's channels and the device's ability to maintain liquid ink may also present possibilities of patterning with species larger than molecules (such as nanoparticles) or with ink molecules that have a higher solubility in solvents. Particularly, the high compliance of the core tip relative to the volcano shell structure as noted in the induced deformation during SEM observation of dry tips (figure 3(*b*)) is also helpful in preventing clogging of the probe orifice and mechanically aids the transfer of larger species from the volcano cavity to the substrate (rapidograph mode of writing). This high compliance also suggests that with a wet cavity, the core tip is unstable in the center of the volcano structure and chooses an off-center position, touching the volcano shell, due to capillary forces. While the core compliance eases the writing process, it may be detrimental to alignment accuracy, resulting in a tolerance about the size of the probe cavity. If this is the case, as with calligraphic quills, a variety of NFP types need to be developed: some for high positioning accuracy and precision writing, with sharp and stiff probes, and others for high writing reliability and large surface coverage to create larger dots or lines, with compliant tips but reduced positioning accuracy and fine writing capability. The different types of probes could eventually be integrated on the same chip, together with tips for different functions (e.g. imaging). Independent actuation and sensing of these probes would be desirable; however this would lead to higher cost probe arrays, justified only by an increase in the lifetime of the chip. The present NFP chip was designed with these future developments in mind. The cantilever and chip body, as well as the processing sequence, allow for the integration of a PZT actuator, while the wear resistance of the probe can be increased by using SiC or diamond instead of silicon nitride for the first layer which forms the probe core.

5. Conclusions

A new generation of the nanofountain probe chip was developed, containing a linear array of 12 cantilever probes with integrated microfluidic channels and ink-dispensing volcano-shaped tips, fed by two on-chip reservoirs. The improvements upon the former device are parallel writing capability, increased probe sharpness and uniformity, better sealing of the microfluidic structure and capability of two-ink writing. The microfabrication consists of standard processes, involving external molding of silicon nitride on convex Si tips, a sacrificial layer technique and DRIE for the release of structures. The writing capabilities of the device were tested with several individual inks; parallel writing with two different inks was also demonstrated. The device is currently in use for biomolecule patterning in assay applications. Future developments include the integration of independent probe actuation, the integration of low wear materials and the investigation of long-range writing capabilities.

Acknowledgments

This work was supported primarily by the Nanoscale Science and Engineering Initiative of the National Science Foundation under NSF Award Number EEC-0118025. We thank Professor Chad Mirkin and his research group for many insightful discussions. The microfabrication was performed in part at the Cornell NanoScale Facility, a member of the National Nanotechnology Infrastructure Network, which is supported by the National Science Foundation (Grant ECS 03-35765). The authors acknowledge the Materials Processing and Crystal Growth Facility (MPCGF) of Northwestern University, Northwestern University Atomic and Nanoscale Characterization Experimental Center (NUANCE) and the Electron Microscopy Center (EMC) of Argonne National Laboratory for the fabrication and characterization facilities.

References

[1] Kim K-H, Moldovan N and Espinosa H D 2005 A nanofountain probe with sub-100 nm molecular writing resolution *Small* **1** 632–5
Kim K-H, Ke C, Moldovan N and Espinosa H D 2003 *Proc. Society of Experimental Mechanics Ann. Conf. (Charlotte, NC, 2–4 June, 2003)* pp 235–8
Kim K-H, Ke C, Moldovan N and Espinosa H D 2003 *Materials Research Society Symp. Proc.* vol 782, pp A5.56.1
[2] Moldovan N, Kim K-H and Espinosa H D 2006 Design and fabrication of a novel microfluidic nanoprobe *J. Microelectromech. Syst.* **15** 204–13
[3] Lewis A, Kheifetz Y, Shambrod E, Radko A and Khatchatryan E 1999 Fountain pen nanochemistry: atomic force control of chrome etching *Appl. Phys. Lett.* **75** 2689–91
[4] Deladi S, Tas N R, Berenschot J W, Krijnen G J M, de Boer M J, de Boer J H, Peter M and Elwenspoek M C 2004 Micromachined fountain pen for atomic force microscope-based nanopatterning *Appl. Phys. Lett.* **85** 5361–3
[5] Piner R D, Zhu J, Xu F, Hong S and Mirkin C A 1999 'Dip-pen' nanolithography *Science* **283** 661–3
Hong S, Zhu J and Mirkin C A 1999 A new tool for studying the *in situ* growth processes for self-assembled monolayers under ambient conditions *Langmuir* **15** 7897
[6] Jang J, Hong S, Schatz G C and Ratner M A 2001 Self-assembly of ink molecules in dip-pen nanolithography: a diffusion model *J. Chem. Phys.* **115** 2721–9
[7] Weeks B L, Vaughn M W and DeYoreo J J 2005 Direct imaging of meniscus formation in atomic force microscopy using environmental scanning electron microscopy *Langmuir* **21** 8096–8
[8] Salaita K, Lee S W, Wang X, Huang L, Dellinger T M, Liu C and Mirkin C A 2005 Sub-100 nm, centimeter-scale, parallel dip-pen nanolithography *Small* **1** 940–5
Zhang M, Bullen D, Chung S-W, Hong S, Ryu K S, Fan Z, Mirkin C A and Liu C 2002 A MEMS nanoplotter with high-density parallel dip-pen nanolithography probe arrays *Nanotechnology* **13** 212–7
[9] Service R F 2002 Biology offers nanotechs a helping hand *Science* **298** 2322–3
[10] Hong S, Zhu J and Mirkin C A 1999 Multiple ink nanolithography: toward a multiple-pen nano-plotter *Science* **286** 523–5
[11] Xu J, Lynch M, Huff J L, Mosher C, Vengasandra S, Ding G and Henderson E 2004 Microfabricated quill-type surface patterning tools for the creation of biological micro/nano arrays *Biomed. Microdevices* **6** 117–23
Vengasandra S, Lynch M, Xu J and Henderson E 2005 Microfluidic ultramicroscale deposition and patterning of quantum dots *Nanotechnology* **16** 2052–5
Xu J, Lynch M, Nettikadan S, Mosher C, Vegasandra S and Henderson E 2006 Microfabricated "biomolecular ink cartridges"—surface patterning tools (SPTs) for the printing of multiplexed biomolecular arrays *Sensors Actuators* B **113** 1034–41
[12] Cai Y and Ocko B M 2005 Electro pen nanolithography *J. Am. Chem. Soc.* **127** 16287–91
[13] Kim K-H, Moldovan N, Ke C, Espinosa H D, Xiao X, Carlisle J and Auciello O 2005 Novel ultrananocrystalline diamond probes for high resolution low-wear nanolithographic techniques *Small* **1** 866–74
[14] Kim K-H, Sanedrin R, Lee W, Moldovan N, Mirkin C A and Espinosa H D 2006 Direct delivery and submicron patterning of DNA by nanofountain probe *Adv. Mat.* submitted
[15] Rosner B and Eby R 2004 Introduction to DPN patterning with parallel, multi-pen arrays *Nanoink Technical Note* http://www.nanoink.net/docs/appnotes/appnotes_multiprobe.pdf
[16] Sheehan P E and Whitman L J 2002 Thiol diffusion and the role of humidity in 'dip pen nanolithography' *Phys. Rev. Lett.* **88** **15** 156104-1–4